Towards a Digital Temporal Thermal Comfort Model: Integrating Field Measurements and Geospatial Analysis for Urban Microclimate Assessment in Rabat, Morocco

Chaimaa Delasse [1,2], Rafika Hajji [1], Tania Landes [2], Hélène Macher [2], Pierre Kastendeuch [3], Georges Najjar [3]

[1] College of Geomatic Sciences and Surveying Engineering, Institute of Agronomy and Veterinary Medicine (IAV), Rabat 6202, Morocco - (c.delasse, r.hajji)@iav.ac.ma
[2] University of Strasbourg, INSA Strasbourg, CNRS, ICUBE UMR 7357 Laboratory, TRIO Team, 67000 Strasbourg, France - (chaimaa.delasse, tania.landes, helene.macher)@insa-strasbourg.fr
[3] University of Strasbourg, Faculty of Geography and Planning, CNRS, ICUBE UMR 7357 Laboratory, TRIO Team, 67000 Strasbourg, France – (kasten, georges.najjar)@unistra.fr

Keywords: Thermal comfort, urban microclimate, 3D urban modelling, mobile acquisition, UTCI.

Abstract

Urban environments face increasing challenges related to thermal discomfort and heat stress due to climate change and rapid urbanization. This study presents a methodology for developing a 4D digital thermal comfort model by integrating time-series pedestrian-level microclimate measurements with a 3D urban model. A mobile field campaign in Rabat, Morocco, collected air temperature, relative humidity, wind speed, and black globe temperature at 22 sampling points over 9 summer days. These measurements were used to calculate the Universal Thermal Climate Index (UTCI). A detailed 3D urban model was created from laser scanning data, featuring Level of Detail 3 (LoD3) for buildings and trees of interest. UTCI point measurements were spatially interpolated using Empirical Bayesian Kriging 3D combined with shading analysis. The interpolated hourly 3D UTCI maps were combined into a voxel dataset through an automated Python workflow, enabling dynamic visualization of thermal comfort evolution. Results revealed distinct diurnal patterns with UTCI values ranging from 17°C (no thermal stress) to 43°C (very strong heat stress), with relatively consistent spatial patterns. Vegetation demonstrated significant cooling effects, with broad-canopied species providing 3-5°C UTCI reduction compared to unshaded areas, while tall palm trees offered minimal cooling, as expected. Interestingly, some vegetation areas exhibited complex thermal behaviour, appearing slightly warmer during morning and evening periods. The approach provides insights into the temporal dynamics of pedestrian-level thermal comfort, establishing a promising foundation for climate-responsive urban planning interventions in Moroccan cities.

1. Introduction

Urban environments face increasing challenges related to thermal discomfort and heat stress, exacerbated by climate change and rapid urbanization. Conventional urban planning approaches typically operate at broader spatial scales with limited temporal resolution, making it difficult to capture the variations in thermal conditions experienced at the pedestrian level. Recent advancements in 3D modelling and geospatial technologies have created opportunities for more sophisticated approaches to urban thermal comfort (TC) representation at a micro-scale. The gap between 3D urban modelling capabilities and actionable TC insights represents a significant opportunity for research and practical application. Urban planners, architects, and policymakers require tools that combine spatial precision with environmental sensitivity to design thermally resilient public spaces that offer comfortable conditions to their dwellers.

In this context, the present study aims to develop a digital 4D TC model that integrates mobile pedestrian-level measurements with 3D urban modelling. Particularly, the Universal Thermal Climate Index (UTCI) was selected as it is considered as a comprehensive bioclimatic index that characterizes how humans physiologically respond to the outdoor thermal environment. It considers the combined effects of air temperature, humidity, wind speed, and radiation. Unlike simple indices, UTCI is based on advanced human thermoregulation modelling and provides a temperature-equivalent measure that is interpretable across diverse climatic contexts (Blazejczyk et al., 2012).

The mobile approach to TC assessment enables broader spatial coverage with limited equipment. Mobile systems can efficiently map thermal conditions across multiple locations during the same time period, providing comparable data under theoretically identical weather conditions. Additionally, mobile measurements taken at pedestrian height better represent the actual thermal environment experienced by city dwellers, providing more relevant data for human-centred urban design. These capabilities make mobile approaches particularly valuable for understanding the spatial patterns of urban TC.

The primary objectives of this research are to:

- Develop a methodology for collecting and integrating pedestrian-level UTCI data with 3D urban models
- Assign a time dimension to the 3D model that takes diurnal variations into account, thus making it a 4D model
- Use the resulting 4D UTCI model to analyse TC variations in the studied area

The remainder of this paper is structured as follows: Section 2 reviews relevant literature on mobile urban TC assessment, particularly in the Moroccan context, as well as existing approaches to represent environmental measurements on 3D models. Section 3 details the data collection protocol. Section 4 presents the methodology employed for model development. Section 5 presents results of the model analysis in the study area. Finally, Section 6 concludes with a summary of findings, discusses the potential implications for urban planning and recommendations for future works.

2. Related works

Research on urban TC assessment has developed across multiple methodological approaches over recent decades. Several innovative mobile monitoring systems have emerged, such as the backpack-mounted CityFeel (Gallinelli et al., 2017), which

addresses limitations of static measurement stations through pedestrian-level "climatic urban walks". This approach captures the multisensory nature of TC by measuring not only standard parameters but also multidirectional radiant temperature, thermal turbulence, and air quality indicators that affect human perception in dynamic urban environments.

In order to maintain sensor positioning at pedestrian height while eliminating potential direct body heat influence on the instruments, mobile measurement carts can be utilized. Klok et al. (2018) conducted simultaneous measurements at different urban typologies (shaded and sunlit areas in parks, streets, squares, and near water bodies) to quantitatively assess the cooling effects of different urban design elements. Their findings confirmed the dominant role of shading in urban TC, with Physiological Equivalent Temperature (PET) reductions of 12-22°C in shaded spaces compared to sunlit areas.

The references found in the literature, relating to thermal comfort and urban planning in Morocco, mainly concern simulation tools at different scales. Numerical modelling approaches include Computational Fluid Dynamics (CFD) simulations for microclimate analysis using ENVI-met (Ouali et al., 2019; Ouali et al., 2023) and Local Climate Zone (LCZ) classification for urban thermal pattern mapping (Ouali, 2023). More recently, these simulation approaches are complemented by field studies using mobile weather stations and continuous monitoring campaigns (Maouni et al., 2023). The spatial scales range from micro-level studies examining urban canyons and specific vegetation effects (Johansson, 2006), to neighbourhood-scale analyses of different urban morphologies (Ouali et al., 2023), to city-wide assessments of Urban Heat Island (UHI) effects and air quality (Maouni et al., 2023).

These assessment methodologies generate valuable TC data. However, the transformation of point-based field measurements or simulation outputs into comprehensible 3D visualizations represents a critical challenge. Several integration methodologies have been explored to represent environmental measurements on 3D models. Texture mapping is a common technique that projects 2D data maps onto 3D geometries, enabling the visualization of surface properties such as temperature (Natephra et al., 2017). However, texture mapping is limited in its ability to capture the depth and volumetric nature of 3D spatial data. Volume rendering addresses this limitation by treating spatial data as a 3D scalar field (Marie et al., 2024). This allows for the visualization of variations and the calculation of new parameters (Zhang and Liu, 2021), providing insights that are not possible with texture mapping techniques.

Voxelization is a specific implementation of volume rendering that discretizes the 3D space into a regular grid of volumetric elements, or voxels. Each voxel can store multiple data attributes, enabling the representation of complex 3D patterns and efficient computation. Recent studies have demonstrated the value of voxel-based approaches for enhancing environmental modelling and visualization in urban contexts. Gabriel et al. (2021) developed a methodology for efficient calculation of annual shading using pre-processed 3D "shading voxels" for tree geometries. Similarly, Ridzuan et al. (2024) showcased the applicability of voxelization techniques for traffic noise visualization and wind flow simulation. They integrated 3D kriging interpolation with voxels to model noise levels on building facades and generated voxel-based building models to simplify CFD simulations.

Particularly, the Network Common Data Form (NetCDF) is a powerful volumetric data format for handling multidimensional scientific data (Rew and Davis, 1990). 3D NetCDF ability to integrate time-series information with spatial coordinates makes it suitable for representing environmental data that varies across both space and time.

The integration of the temporal dimension in 3D modelling has evolved significantly to enable more comprehensive analysis of dynamic environmental phenomena. Natephra et al. (2017) developed a methodology for creating 4D thermal models by integrating time-stamped thermal data into Building Information Modelling (BIM), allowing for visualization of thermal patterns over time by using a sidebar control in Rhinoceros software. Similarly, the thermal model developed by Marie et al. (2024) supports time-based visualization of surface temperature changes using Paraview software, which handles scalar fields with temporal dimensions.

The present research extends the voxel-based approach using 3D NetCDF by incorporating temporal aspects on TC analysis using the UTCI to visualize diurnal variations in outdoor comfort conditions. Additionally, this work represents one of the first applications of mobile in-situ microclimate measurements combined with 3D visualization techniques in Rabat, Morocco.

3. Data collection

The study area is located in a residential area in Hay Riad, Rabat, Morocco, covering three streets characterized by distinct vegetative configurations (Figure 1). These configurations include: (1) streets with mature trees on both sides, (2) streets with vegetation on only one side, and (3) streets with no tree cover. The vegetation varies across the study area, featuring broad-canopied tree species, palm trees, and grassy areas, providing a diverse range of shading conditions and potential vegetative cooling effects.

3.1 Geometric data

A laser scanning campaign was conducted to obtain the point cloud of the study area. Based on this data, a 3D model was created (Figure 1) following the process presented below (section 4.1).

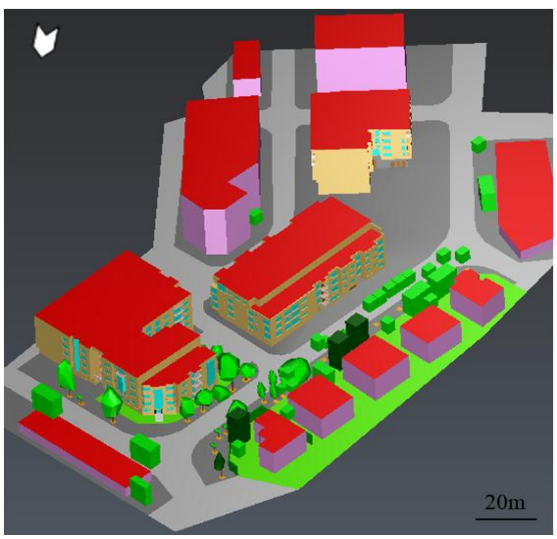

Figure 1. 3D model of the study area reconstructed from laser scanning data.

3.2 Thermal comfort (TC) data

A microclimate data collection campaign was carried out in the study site during the summer of 2024, measuring air temperature, relative humidity, air velocity and black globe temperature. Measurements were conducted using the Delta OHM HD 32.3 data logger (Figure 2), along with the corresponding sensor probes (Figure 3). The system was positioned at a height of 1.1 meters above ground level in accordance with ISO 7726 (1998) standards, representing the centre of gravity of a standing human body. The equipment was mounted on a range pole with a supporting strut to ensure stability and to maintain distance from the operator, preventing body heat interference with measurements.

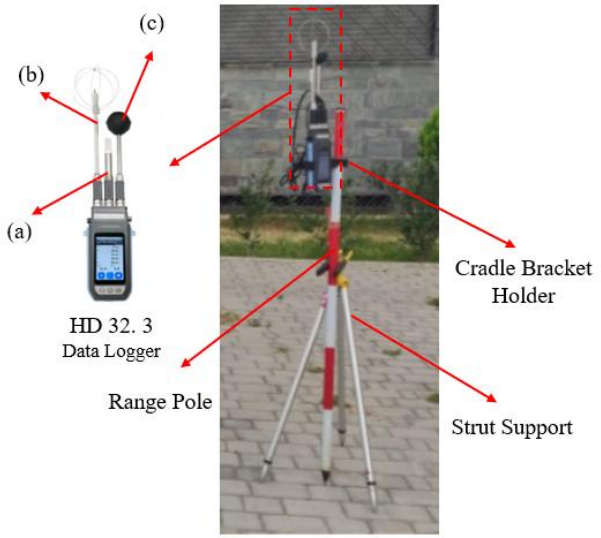

Figure 2. TC measurement system.

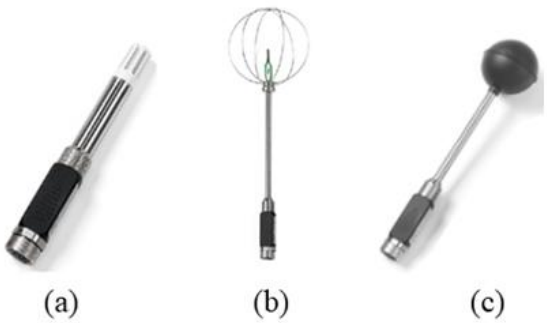

Figure 3. Sensor probes for: (a) air temperature (Ta) and relative humidity (RH), (b) air velocity (va) and (c) black globe temperature.

	(a) Ta and RH	(b) va	(c) black globe temperature
Accuracy	Ta = 1/3 DIN[1] RH = ±2% (90 to 100% RH)	± (0.05 + 0.5%) m/s	1/3 DIN
Resolution	0.1 °C; 0.1 RH	0.01 m/s	0.1 °C
Range	Ta= -40 to 100 °C; HR = 0 to 100 %	0.05 to 5 m/s 0 to 80 °C	-30 to 120 °C

Table 1. Sensor technical specifications (Source: Senseca Italy Srl).

To complement the TC measurement system, an additional temperature and humidity probe was installed inside a meteorological shelter mounted on a survey rod at a height of 1.4 meters to minimize direct solar radiation and wind variation effects. This system ensures reliable data collection and comparability with the TC station values.

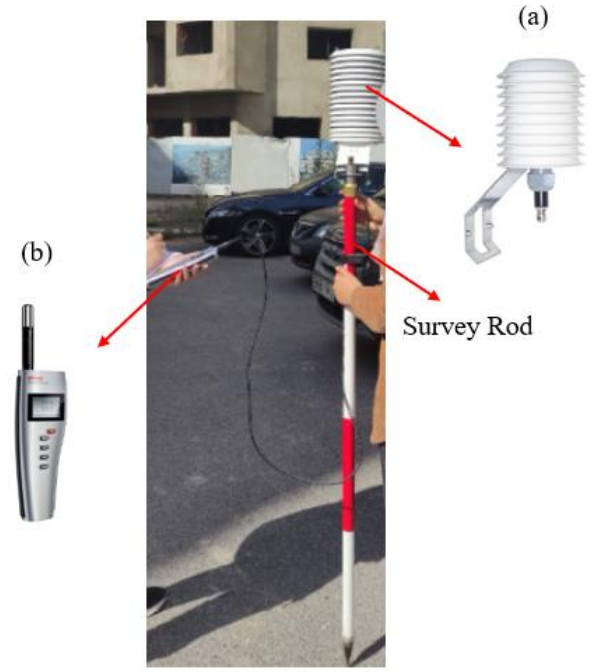

Figure 4. Additional temperature and humidity measurement setup with (a) temperature and humidity sensor housed in radiation shield and (b) HygroPalm HP21 handheld data reader

Measurements were collected at 22 sampling points over a period of 9 days, with observations recorded at 1.5-hour intervals between 7:00 AM and 7:00 PM local time. During each measurement session, the operator systematically recorded the shading conditions at every sampling point, noting whether the location was fully exposed to sunlight, partially shaded, or completely shaded by surrounding buildings or vegetation. This documentation was crucial because mean radiant temperature (Tmrt) is highly sensitive to solar exposure conditions (Thorsson et al., 2007). Tmrt represents the uniform temperature of an imaginary enclosure in which radiant heat transfer from the human body equals the radiant heat transfer in the actual non-uniform enclosure. It can vary significantly within short distances

[1] DIN = Deutsches Institut für Normung; standards for sensor accuracy

depending on solar access. By recording the contextual shading conditions, we could better interpret variations in TC indices and establish more accurate relationships between the urban geometry, vegetation patterns, and resulting thermal environments.

4. Methodology

The proposed methodology aims to develop a 4D digital UTCI model based on the acquired data. The workflow consists of four primary steps: (1) 3D modelling from point cloud data, (2) calculation of UTCI values from field measurements, (3) 3D kriging interpolation, and (4) temporal visualization. Figure 5 describes the general methodology flowchart.

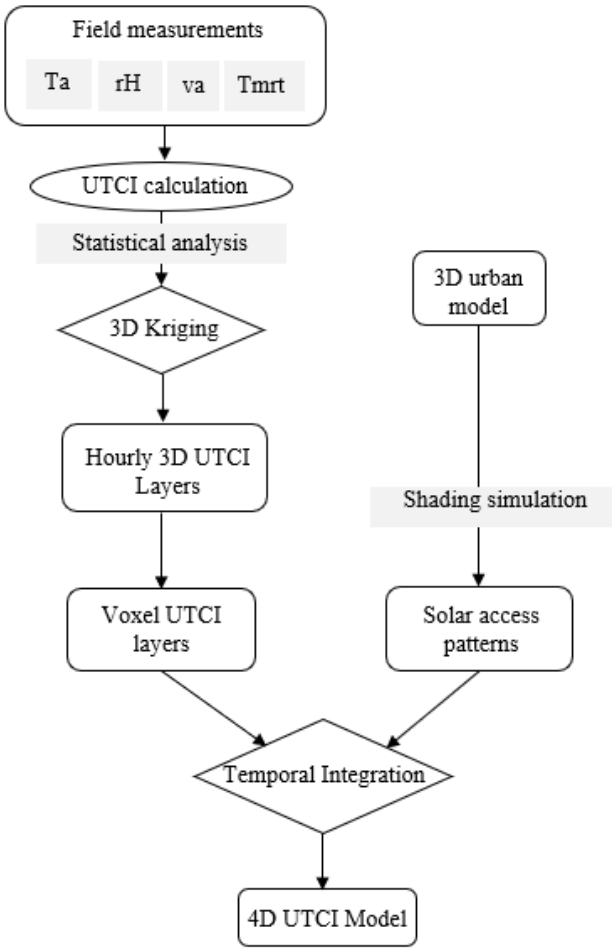

Figure 5. Methodology flowchart proposed for creating a temporal UTCI Model

4.1 3D modelling

A detailed urban 3D model (Figure 1) was first created based on point cloud data, featuring LoD3 buildings (modelled in Revit from Autodesk) and trees (modelled using a specifically designed MATLAB program). This is to achieve more accurate shading simulation and to better identify and explain spatial TC variations throughout the urban environment. Additional urban elements, which were more distant from the areas of interest, were modelled in LoD1 (using 3D Reshaper from Leica Geosystems), creating a virtual environment for analysis.

4.2 UTCI Calculation

Using the microclimate data collected in the field campaign, UTCI values were computed for each of the 22 sampling points. The UTCI calculation followed the approach recommended by Bröde (2021), using the lookup table method which provides more accurate results compared to the polynomial regression approach.

The calculation procedure required four input parameters: Ta, Tmrt, va, and RH. Tmrt values were directly obtained from the TC measurement station using the black globe thermometer. Wind speed measurements were adjusted to the meteorological reference height of 10m using the logarithmic formula provided by Bröde et al. (2012), as shown in eq. (1).

$$va = va_{xm} \cdot LOG(10/0.01) / LOG(x/0.01) \qquad (1)$$

where vaxm is the wind speed measured at height x meters above ground level. All measured parameters were verified to fall within the valid range for UTCI calculation: -50°C ≤ Ta ≤ +50°C, -30°C ≤ Tmrt - Ta ≤ +70°C, 0.5 m/s ≤ va ≤ 30.3 m/s, and 5% ≤ RH ≤ 100% (with pa < 50 hPa).

UTCI values were calculated using a Python implementation of the original Fortran code published by the authors. The calculated UTCI values were then interpreted using the official assessment scale, which was adapted according to the limit values encountered in the field measurements, ranging from 17°C (no thermal stress) to 43°C (very strong heat stress).

4.3 3D Kriging Interpolation

Prior to interpolation, exploratory statistical analysis was conducted to understand the distribution characteristics of the UTCI dataset. This analysis included tests for normality, trend assessment, and spatial autocorrelation evaluation using ArcGIS Pro's Global Moran's I. Given the limited number of sampling points (22 points per period), data was pooled across similar time periods: mornings, afternoons and evenings. The UTCI values showed moderate positive spatial autocorrelation, confirming the suitability of kriging-based interpolation methods.

Multiple kriging methods were evaluated, including Ordinary Kriging, Universal Kriging, and Empirical Bayesian Kriging 3D (EBK3D). Cross-validation using the leave-one-out method was performed to compare prediction accuracy. EBK3D with the K-Bessel semi variogram model demonstrated superior performance with the lowest root mean square error (RMSE = 1.23°C). Additionally, EBK3D accounts for uncertainty in semi variogram estimation through simulation, reduces smoothing effects at measurement locations and handles non-stationary data effectively through local model fitting (Krivoruchko., 2012).

Inherently, UTCI exhibits abrupt variations in shaded zones that challenge spatial interpolation methods. The approach was therefore combined with shading analysis to better account for this issue. The interpolation was performed separately for each hour of measurement, creating a series of three-dimensional UTCI maps. These hourly 3D models were then overlaid with shading analysis results to investigate the impact of solar access patterns. Though interpolation has limitations for variables with sharp spatial gradients like UTCI, this methodology attempts to address this by explicitly incorporating shadow boundaries in the analysis framework.

4.4 Temporal visualization

The temporal dimension was incorporated by combining the hourly layers into a NetCDF voxel dataset. This enables dynamic visualization and analysis of TC evolution throughout the study period. A Python script was developed to automate the workflow from the extraction of hourly 3D UTCI layers through conversion to NetCDF voxel format to temporal integration using ArcGIS Pro time slider functionality. This automation ensured consistent processing across all time periods and facilitated rapid regeneration of visualizations.

The solar shading analysis was also performed using ArcGIS Pro based on the 3D model. The resulting shadow patterns were then synchronized with the interpolated UTCI data within a unified visualization framework. The visualization system supports multiple modes of analysis including temporal animations depicting the progression of TC zones throughout the day, interactive queries allowing point-based and region-based TC assessment, and comparative visualization of identical locations under different solar exposure conditions.

5. Results

The voxel representation of interpolated UTCI values is structured as a 150 x 100 m horizontal grid with 2 m vertical resolution, allowing for analysis of TC conditions throughout the study area.

The following sections present (1) the temporal and spatial UTCI distribution across the dataset, (2) urban morphology and heat stress patterns, (3) vegetation influence, and (4) a comparative analysis, evaluating UTCI differences between two measurement dates.

5.1 Temporal and Spatial UTCI Distribution

Analysis of diurnal UTCI values on July 24, 2024 (Figure 6), reveals distinct temporal fluctuations. During the morning period at 07:00 AM (Figure 6.a), UTCI values predominantly ranged from 23°C to 28°C, mainly falling within the zone of comfortable thermal conditions. As solar exposure increased throughout the day, UTCI values escalated to peak measurements between 31°C and 43°C during the afternoon (Figure 6.b), crossing into moderate, strong, and very strong heat stress categories. This diurnal variation represents an average increase of 14°C in UTCI values from morning to afternoon. The evening period (Figure 6.c) reveals a distinctive shift in the UTCI distribution pattern compared to the afternoon peak. By this time, UTCI values have significantly moderated across most of the study area, returning to the slight heat stress range. This temporal transition is due to the cooling effect that occurs as direct solar radiation decreases. The thermal hotspots that were prominent during the afternoon appear as small residual areas of moderate heat stress persisting in the northeast portion of the site (Figure 6.c.(A)).

The visualization also highlights the influence of urban geometry on thermal patterns even after sunset. The central corridor between building blocks maintains slightly higher UTCI values than surrounding areas, suggesting reduced ventilation in this semi-enclosed urban canyon that likely slows the cooling process. Conversely, areas at the periphery of the study site show accelerated cooling, benefiting from greater exposure to evening airflow.

This evening thermal pattern underscores the dynamic nature of urban microclimate throughout the diurnal cycle and emphasizes how different urban features can influence both daytime heating and evening cooling processes. The relatively quick transition to more comfortable conditions by early evening also indicates the potential importance of timing for outdoor activities in this climate context, with significantly improved TC available shortly after sunset.

5.2 Urban Morphology and Heat Stress Patterns

The primary hotspot with highest UTCI values was observed in the northwest portion of the study area (Figure 6.b.(B)), where UTCI values consistently reached above 38°C during peak afternoon hours. This finding is consistent with the fact that, in this area, shading is limited, notably due to low vegetation cover.

An additional hotspot was identified in the central-eastern section where built density is higher, but street orientation allows for extended solar exposure during the afternoon period. In this area, UTCI values averaged 36°C between 1:00 PM and 3:00 PM, approximately 2°C lower than the northwest hotspot but still within the strong heat stress category.

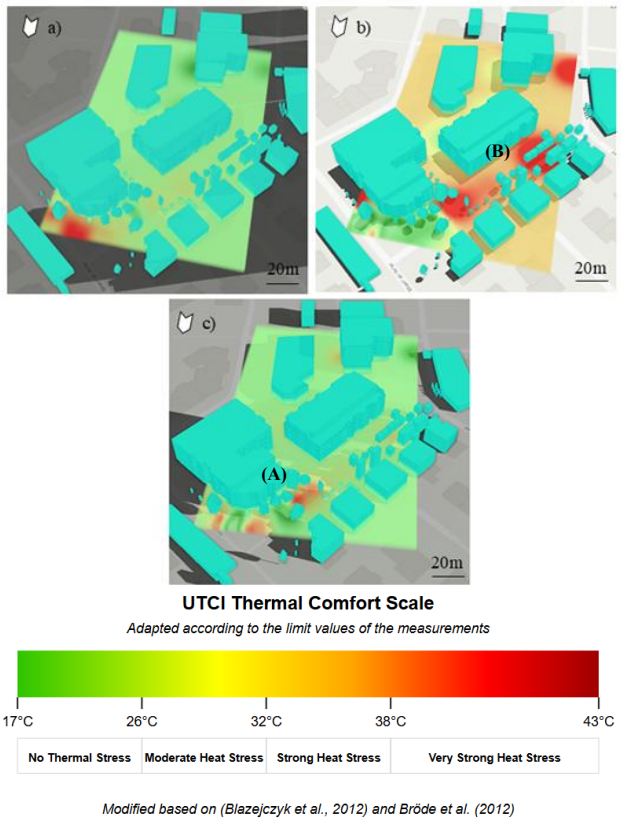

Figure 6. UTCI distribution (July 24, 2024); a) 07:00 AM b) 2:30 PM c) 7:00 PM

5.3 Vegetation Influence

The impact of vegetation is also interesting to observe. It varies depending on tree type and tree configuration. Areas with linear tree clusters maintained UTCI values 3 to 5°C lower than similar adjacent unshaded spaces throughout the afternoon period. This cooling effect was most evident beneath broader-canopied tree species, primarily *Eucalyptus* and *Ficus* species, which created consistent cool islands with UTCI values remaining below 32°C even during peak solar hours.

In contrast, the tall palm trees (*Phoenix dactylifera*, modelled in LoD1) provided minimal cooling effect due to their sparse canopy structure, with areas beneath these trees showing strong heat stress.

Interestingly, the area containing thicker-trunked palms with fuller crown of fronds (*Phoenix canariensis*) and coniferous trees (mainly *Pinus* and *Juniperus* species) on grassy areas demonstrated intermediate cooling performance, with UTCI reductions of 1-2°C compared to unshaded areas.

5.4 Comparative Analysis Between Two Measurement Dates

A comparative analysis between the hottest day (July 24, 2024, Figure 6) and the coldest day (August 7, 2024, Figure 7) of the measurement campaign reveals differences in TC patterns while maintaining relatively consistent spatial relationships.

The morning period (Figures 6.a and 7.a) shows small differences in baseline conditions between the two days. On July 24, UTCI values already showed areas of slight heat stress, whereas August 7 presented predominantly comfortable conditions across most of the study area. This difference (approximately 2-3°C lower UTCI values on August 7) suggests the importance of overnight cooling and potentially different synoptic weather conditions between the two dates.

Peak afternoon conditions (Figures 6.b and 7.b) show the most contrast between the two days. July 24 exhibited extensive areas of moderate to strong heat stress with UTCI values exceeding 38°C in hotspots. In contrast, August 7 displayed a significantly moderated thermal environment, with predominantly slight to moderate heat stress and UTCI values typically 4-6°C lower than those observed on July 24.

Despite these absolute differences, the spatial pattern of heat distribution remains relatively consistent, with similar hotspot locations appearing on both days, particularly in the northwest portion and along west-east oriented corridors (Figure 7.b.(B)).
The evening period (Figures 6.c and 7.c) shows a convergence in thermal conditions between the two days, with both dates returning to predominantly comfortable conditions. However, the persistent hotspot in the northeast corner (Figure 6.c.(A) and 7.c.(A)) remains visible on both days, though with reduced intensity on August 7. This consistent feature suggests that this location's thermal properties are likely influenced by fixed urban characteristics.

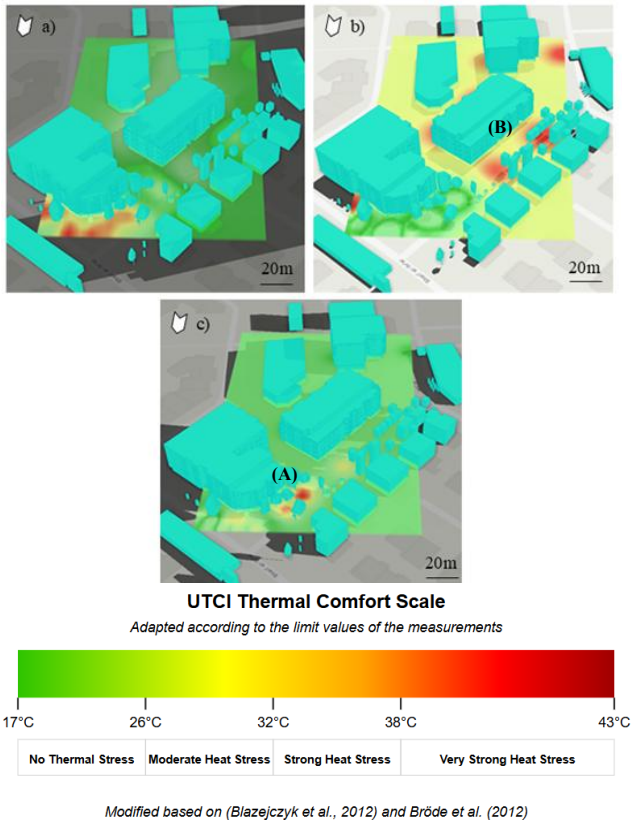

Figure 7. UTCI distribution (August 07, 2024); a) 07:00 AM b) 2:30 PM c) 7:00 PM

Vegetation effects remain consistent across both days, with vegetated areas maintaining their cooling advantage relative to surrounding spaces. On the cooler day (August 7), the cooling effect of vegetation is proportionally more significant in creating comfortable microclimates, despite the overall lower UTCI values. Interestingly, slight hotspots were consistently observed near areas with broad-canopied vegetation during both morning and evening periods on both the hottest and coldest days of the measurement campaign.

These findings demonstrate that while absolute UTCI values vary significantly between extreme days, the relative spatial patterns of TC remain largely consistent. This suggests that targeted urban design interventions would provide benefits across varying weather conditions, though their relative importance may be heightened during extreme heat events.

6. Discussion and Conclusion

The observed phenomenon of slight hotspots near broad-canopied vegetation during morning and evening periods presents an interesting point. This pattern can be explained by several potential mechanisms. First, dense tree canopies may trap longwave radiation emitted from the ground surface during nighttime and early morning hours, reducing radiative cooling compared to open areas. This canopy-induced reduction in nocturnal cooling has been documented in previous studies (Bowler et al., 2010; Armson et al., 2012) and appears to be particularly pronounced in the broad-leaved evergreen species present in the study area.

Another potential explanation may be that these vegetated areas experience a delayed thermal response compared to surrounding open spaces, warming more slowly in mornings and cooling more gradually in evenings due to the thermal inertia of vegetation biomass and associated soils (Potchter et al., 2006). This would create a more thermally stable microclimate beneath canopies, appearing relatively warmer when surrounding areas are at their coolest, while still providing significant cooling benefits during peak daytime hours.

Additionally, these vegetation clusters may be influencing local air circulation patterns by reducing wind speeds beneath and around the canopy, thereby limiting convective cooling during periods of lower solar radiation. This effect would be most noticeable during transition periods when radiative forcing is minimal but thermal inertia from the previous heating/cooling cycle remains significant.

The soil conditions around these vegetation areas might also contribute to this effect, as irrigation practices in the nighttime/ early mornings could increase soil moisture content, potentially altering the thermal properties of the ground surface and changing its heat storage and release patterns. Higher soil moisture would increase thermal inertia, potentially slowing the cooling process in evening hours and the warming process in morning hours.

The observed thermal patterns appear consistent with Maouni et al. (2023), who found significant temperature variations between areas with different vegetation configurations. Their work in Martil noted that deciduous trees like *Populus nigra* and *Platanus orientalis* created more substantial cooling effects compared to palm species. The importance of species selection emerges with data suggesting that strategic vegetation planning requires consideration of both thermal performance and local ecological conditions. These observations highlight the complex role of vegetation in urban microclimates across the diurnal cycle, suggesting that while broad-canopied trees provide highly beneficial cooling during peak heat periods, their influence on local thermal conditions follows a more nuanced pattern throughout the 24-hour cycle.

In summary, this study demonstrates the feasibility of integrating thermal comfort metrics into 4D urban models, providing a framework for urban microclimate analysis and planning. By focusing on pedestrian-level thermal comfort through systematic field measurements, this approach highlights the potential of combining microclimate measurements with geospatial tools to create more resilient urban environments. This is achieved through identification of critical hotspots, assessment of vegetation cooling effects, temporal mapping of thermal stress periods, and visualization of shade-comfort relationships. This work shows that several factors can significantly mitigate heat stress and improve quality of life in urban environments: a) selecting appropriate species of trees and placing them strategically (as green corridors); b) designing urban layouts that facilitate natural ventilation during evening hours; c) prioritizing shade creation during peak thermal stress periods.

Moreover, the voxel-based 3D thermal modelling approach employed in this study serves as both an analytical tool and a communication medium between researchers, urban planners, and policymakers. By visualizing complex microclimatic data in an intuitive spatial format, it enables evidence-based decision making that balances thermal performance with other urban design considerations.

The TC data collected in this study will serve as a ground truth base to compare with simulation results, specifically using LASER/F (LAtent, SEnsible, Radiation / Fluxes) developed by Kastendeuch et al. (2006). LASER/F is a thermoradiative-based microclimate simulation software capable of simulating the effect of buildings and vegetation on the thermal dynamics of the studied area in a 3D environment. Future work will extend this methodology to include simulation testing of different urban design scenarios, such as modified building configurations, strategic vegetation placement, and alternative material selections. Additionally, incorporating seasonal variations beyond the summer period would provide a more comprehensive understanding of year-round TC dynamics. Increasing the number of sampling points both horizontally and vertically would also enhance the spatial accuracy of the resulting model.

7. Acknowledgements

The authors would like to thank the TOUBKAL PHC (Toubkal 48579TJ) for its financial support. Special appreciation is extended to S. Aitbenhammou, H. Elmokhi and S. Boudarbala, Master's graduates in Geomatics from the Institut Agronomique et Vétérinaire Hassan II (IAV Hassan II), for their contribution to this work.

8. References

Armson, D., Stringer, P., Ennos, A. R., 2012. The effect of tree shade and grass on surface and globe temperatures in an urban area. Urban Forestry & Urban Greening, 11(3), 245-255. https://doi.org/10.1016/j.ufug.2012.05.002.

Blazejczyk, K., Epstein, Y., Jendritzky, G., Staiger, H., Tinz, B., 2012. Comparison of UTCI to selected thermal indices. International Journal of Biometeorology, 56, 515-535, https://doi.org/10.1007/s00484-011-0453-2.

Bröde, P., Fiala, D., Błażejczyk, K., Holmér, I., Jendritzky, G., Kampmann, B., Tinz, B., Havenith, G., 2012. Deriving the operational procedure for the Universal Thermal Climate Index (UTCI). International Journal of Biometeorology, 56(3), 481-494.

Bröde, P., 2021. Issues in UTCI Calculation from a Decade's Experience, in: Krüger, E.L. (Ed.), Applications of the Universal Thermal Climate Index UTCI in Biometeorology. Springer International Publishing, Cham, pp. 13–21. https://doi.org/10.1007/978-3-030-76716-7_2.

Bowler, D. E., Buyung-Ali, L., Knight, T. M., Pullin, A. S., 2010. Urban greening to cool towns and cities: A systematic review of the empirical evidence. Landscape and Urban Planning, 97(3), 147-155. https://doi.org/10.1016/j.landurbplan.2010.05.006.

Gabriel, M., Fellner, J., Reitberger, R., Lang, W., Petzold, F., 2021. Voxel based method for real-time calculation of urban shading studies. In Proceedings of the 12th Symposium on Simulation for Architecture and Urban Design (SimAUD), USC, Los Angeles, CA, USA, pages 15–17, 2021.

Gallinelli, P., Camponovo, R., Guillot, V., 2017. CityFeel – Micro climate monitoring for climate mitigation and urban design. Energy Procedia, 122, 391–396. https://doi.org/10.1016/j.egypro.2017.07.427.

ISO 7726:1998 – Ergonomics of the thermal environment – Instruments for measuring physical quantities, International Organization for Standardization, Geneva, Switzerland, 1998.

Johansson, E., 2006. Influence of urban geometry on outdoor thermal comfort in a hot dry climate: A study in Fez, Morocco, Build. Environ., 41, 1326–1338, https://doi.org/10.1016/j.buildenv.2005.05.022.

Kastendeuch P.P., Najjar G., Ringenbach N., 2006. Modélisation du bilan radiatif et d'énergie d'un canyon urbain à Strasbourg. Climatologie, 3, pp. 25-42.

Klok, L., Rood, N., Kluck, J., and Kleerekoper, L., 2019. Assessment of thermally comfortable urban spaces in Amsterdam during hot summer days, Int. J. Biometeorol., 63, 129–141, https://doi.org/10.1007/s00484-018-1644-x.

Krivoruchko, K. 2012. Empirical Bayesian Kriging: Implemented in ArcGIS Geostatistical Analyst. ESRI: Redlands, CA, USA.

Maouni, Y., Boubekraoui, H., Taaouati, M., Maouni, A., Draoui, M., 2023. Assessment of urban outdoor comfort variation in a northwestern Moroccan city – Toward the implementation of effective mitigation strategies, Ecol. Eng. Environ. Technol., 24, 1–18, https://doi.org/10.12912/27197050/169242.

Marie, E., Lecomte, V., Landes, T., Macher, H., Delasse, C., 2024. Temporal and thermal visualization by fusion of thermal images and 3D mesh. Int. Arch. Photogr. and Remote Sens. Spat. Inf. Sci. XLVIII-2/W8-2024, 319–326, https://doi.org/10.5194/isprs-archives-XLVIII-2-W8-2024-319-2024.

Natephra, W., Motamedi, A., Yabuki, N., Fukuda, T., 2017. Integrating 4D thermal information with BIM for building envelope thermal performance analysis and thermal comfort evaluation in naturally ventilated environments. Build. Environ. 124, 194–208. https://doi.org/10.1016/j.buildenv.2017.08.004.

Ouali, K., El Harrouni, K., Abidi, M. L., Diab, Y., 2019. Analysis of Open Urban Design as a tool for pedestrian thermal comfort enhancement in Moroccan climate, J. Build. Eng., 26, 101042, https://doi.org/10.1016/j.jobe.2019.101042.

Ouali, K. 2023. Assessment of the mixed local climate zones as the best design for future eco-districts in sub-humid climate: A case of Rabat, Int. J. Sustain. Build. Technol. Urban Dev., 14, 3–17, https://doi.org/10.22712/susb.20230002.

Potchter, O., Cohen, P., Bitan, A., 2006. Climatic behavior of various urban parks during hot and humid summer in the Mediterranean city of Tel Aviv, Israel. International Journal of Climatology, 26(12), 1695-1711.

Rew, R. K., & Davis, G. P., 1990. NetCDF: An interface for scientific data access. IEEE Computer Graphics and Applications, 10(4), 76-82. https://doi.org/10.1109/38.56302.

Ridzuan, N., Wickramathilaka, N., Ujang, U., Azri, S., 2024. 3D Voxelisation for Enhanced Environmental Modelling Applications. Pollution 10, https://doi.org/10.22059/poll.2023.360562.1942.

Thorsson, S., Lindberg, F., Eliasson, I., Holmer, B., 2007. Different methods for estimating the mean radiant temperature in an outdoor urban setting. International Journal of Climatology, 27(14), 1983-1993.

Zhang, Y., Liu, C., 2021. Digital Simulation for Buildings' Outdoor Thermal Comfort in Urban Neighborhoods. Buildings 11, 541. https://doi.org/10.3390/buildings11110541.